nature cell biology

A NUDEL-dependent mechanism of neurofilament assembly regulates the integrity of CNS neurons

Minh Dang Nguyen[1,2], Tianzhi Shu[1], Kamon Sanada[1], Roxanne C. Larivière[2,3], Huang-Chun Tseng[1], Sang Ki Park[1], Jean-Pierre Julien[2,3] and Li-Huei Tsai[1,4]

The cytoskeleton controls the architecture and survival of central nervous system (CNS) neurons by maintaining the stability of axons and dendrites. Although neurofilaments (NFs) constitute the main cytoskeletal network in these structures, the mechanism that underlies subunit incorporation into filaments remains a mystery. Here we report that NUDEL, a mammalian homologue of the *Aspergillus nidulans* nuclear distribution molecule NudE, is important for NF assembly, transport and neuronal integrity. NUDEL facilitates the polymerization of NFs through a direct interaction with the NF light-subunit (NF-L). Knockdown of NUDEL by RNA interference (RNAi) in a neuroblastoma cell line, primary cortical neurons or post-natal mouse brain destabilizes NF-L and alters the homeostasis of NFs. This results in NF abnormalities and morphological changes reminiscent of neurodegeneration. Furthermore, variations in levels of NUDEL correlate with disease progression and NF defects in a mouse model of neurodegeneration. Thus, NUDEL contributes to the integrity of CNS neurons by regulating NF assembly.

NudE is a [**AU: please say what kind of protein NudE is**] that is implicated in nuclear distribution during hyphal growth in *A. nidulans*. In contrast, the mammalian homologue of NudE, NUDEL, interacts with Dynein heavy chain (Dhc), 14-3-3ξ, DISC1 and Lis1 — proteins associated with schizophrenia and lissencephaly, respectively[1–5]. During neurodevelopment, NUDEL is expressed in neuronal precursors and migrating neurons. Consistent with the functions of Nud proteins during nuclear distribution in *A. nidulans*, NUDEL (in association with Lis1 and Dhc) is thought to function in nucleokinesis, neuronal migration and corticogenesis. Protection of Cdk5-phosphorylated NUDEL from protein phosphatase 2A activity by 14-3-3ξ binding may be crucial for these events[5]. Interestingly, NUDEL expression peaks in early post-natal stages of CNS development and continues throughout adulthood, suggesting that is has important roles during neuronal maturation and maintenance. Aside from in neurodevelopment, the physiological functions of NUDEL, however, remain unclear[1–3].

NFs constitute the major filamentous network of the neuronal cytoskeleton. They are type-IV intermediate filaments (IF) composed of three subunits: NF-L, NF-M and NF-H (for reviews see refs 6–10). As with NUDEL, the expression of the NF triplet is weak in embryonic CNS tissues but increases significantly in the initial post-natal days[3,4,11,12]. Gene-targeting and transgenic experiments in mice have highlighted a crucial function of NFs in the radial growth and maintenance of myelinated axons, dendritic arborization, axonal transport, nerve conduction and, thus, neuronal architecture, integrity and survival (for reviews see refs 6–10). NFs are obligate heteropolymers *in vivo*, requiring the assembly of the key subunit NF-L together with either NF-M or NF-H in the correct stoichiometry[6–10]. In the absence of NF-L, no filaments are formed[13]. The central rod domain of the NF proteins, which is approximately 300 amino acids in length and contains two coiled-coil sub-domains, is responsible for heterodimerization and the formation of filaments[6–10]. After synthesis in the cytoplasm, a major fraction of soluble NF proteins is rapidly incorporated into the polymeric filamentous network, referred to as the 'insoluble fraction'[14,15]. These filaments move down the axon using both the anterograde kinesin and retrograde dynein/dynactin transport machinery[9,16–20]. In parallel, individual NF subunits that constitute the soluble fraction translocate rapidly along NFs and microtubules[9,21–23].

Despite their abundance and instrumental role in CNS neurons, the molecules and mechanisms underlying the transition of NF subunits into filaments remain undefined[6–10]. Understanding this process might help to unravel fundamental aspects of NF assembly and mechanisms of neuronal death.

RESULTS

NUDEL interacts directly with NF-L at the rod domain and forms soluble complexes with NF-H in the adult mouse CNS

[AU: Please shorten Title to fit on one line.]

The majority of NF proteins assemble in adult mouse CNS tissues rendering them insoluble in NP-40- or Triton X-100-containing lysis buffer; unassembled subunits, however, remained soluble (Fig. 1a). To determine whether NUDEL interacts with soluble unassembled NF subunits, we performed pull-down assays of NF proteins from soluble fractions of spinal-cord lysates using purified glutathione *S*-transferase

[1]Department of Pathology, Harvard Medical School and Howard Hughes Medical Institute, 77 Avenue Louis Pasteur, New Research Building, Room 856-8, MA 02115, USA. [2]Centre for Research in Neuroscience, The Montreal General Hospital Research Institute, 1650 Cedar Avenue, Montréal, Québec, H3G 1A4, Canada. [3]Present address: CHUL Research Center, Department of Anatomy and Physiology, Laval University, 2705 Boulevard Laurier, Sainte-Foy, Québec, G1V 4G2, Canada. [4]Corrrespondence should be addressed to M.D.N. (e-mail: minh-dang_nguyen@hms.harvard.edu) or L.-H.T. (e-mail: li-huei_tsai@hms.harvard.edu)

Published online: XXXX 2004, DOI: 10.1038/ncbXXXX

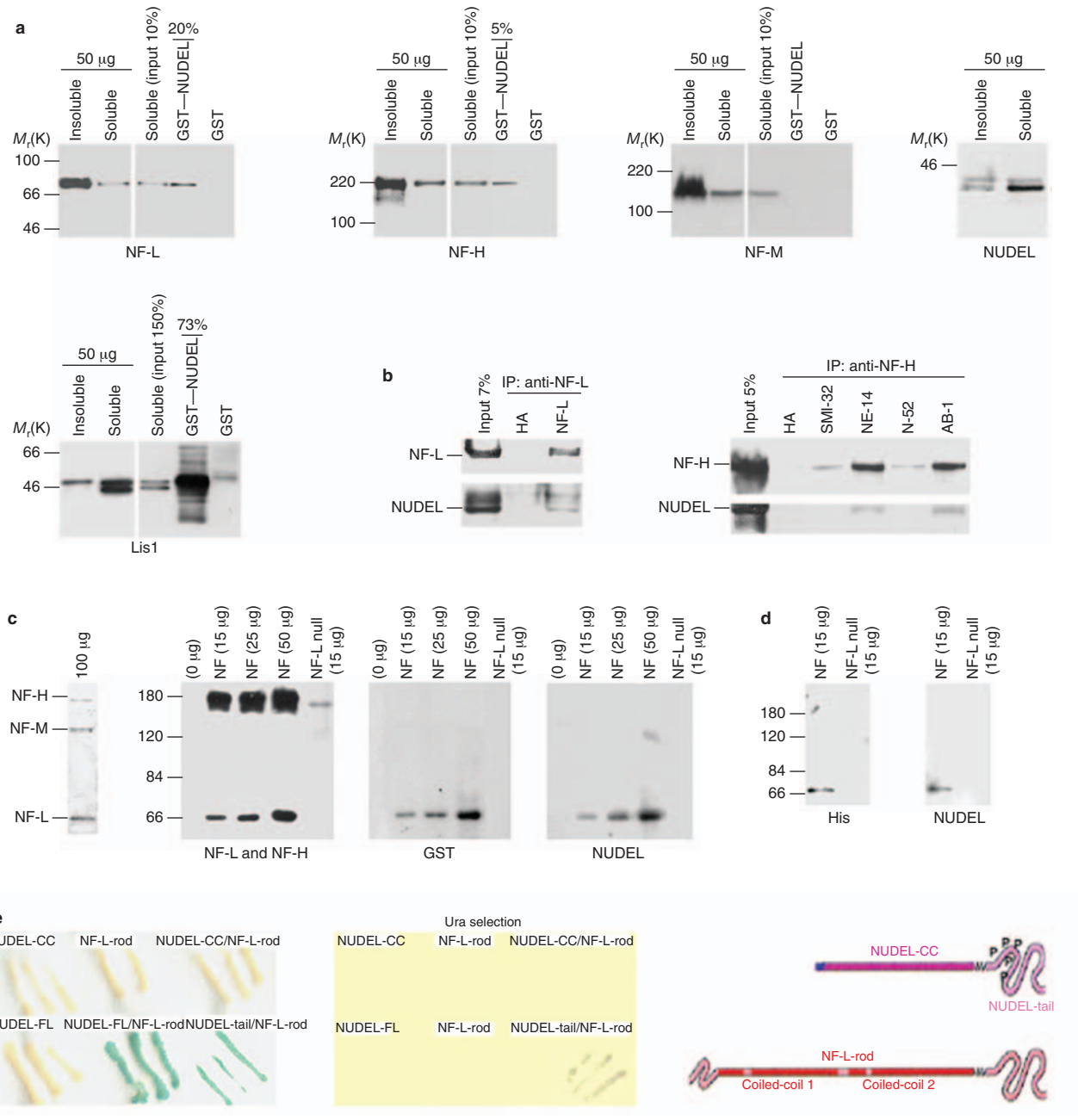

Figure 1 NUDEL interacts directly with NF-L at the rod domain and associates indirectly with NF-H in the soluble fraction of adult mouse CNS. **[AU: Please shorten Title to fit on one line.]** (**a**) GST–NUDEL pulled down NF-L and NF-H proteins, but not NF-M, from soluble fractions of mouse adult spinal cord. GST–NUDEL also pulled down Lis1 (positive control). The amount of pulled down proteins from the soluble fraction is expressed as a percentage. Note that NF proteins are predominantly insoluble, whereas NUDEL and Lis1 are more soluble. (**b**) Co-immunoprecipitation of NUDEL with NF-L and NF-H proteins from mouse brain lysates. NUDEL co-immunoprecipitated with NF-L in the presence of NF-L antibodies (NR 4) **[AU: OK?]**. NUDEL also co-immunoprecipitated with NF-H in the presence of specific monoclonal NF-H antibodies (NE-14 and AB-1). Other NF-H antibodies (SMI-32 and N-52) did not successfully immunoprecipitate NF-H protein. A monoclonal anti-HA antibody was used as a negative control. (**c**) Overlay binding assays using GST–NUDEL and purified NF proteins from adult mice **[AU: OK?]**. A Coomassie gel containing 100 μg of proteins per lane shows the predominance of the three NF subunits in the preparations. The presence of NF subunits was verified by western blot analysis with NF-L and NF-H antibodies. GST–NUDEL (3–5mg ml^{-1}) bound directly to NF-L protein in a dose-dependent manner (15, 25 or 50 μg), but not to NF-M and NF-H proteins as detected with anti-GST monoclonal antibodies or anti-NUDEL antibodies. NF preparations from NF-L-null mice confirmed the specificity of binding to NF-L. Note the decrease of NF-H in NF-L-null mice[13] (wild-type mice, $n = 6$); NF-L-null mice, $n = 3$). (**d**) Overlay binding assays utilizing His–NUDEL and purified NF proteins from adult mice provided evidence for the specific binding of NUDEL to NF-L (wild-type mice, $n = 3$; NF-L-null mice, $n = 3$). (**e**) Definition of the interaction domains of NUDEL and NF-L by the yeast two-hybrid expression system. NUDEL-FL (amino acids 1–345) or NUDEL-tail (amino acids 191–345) interacted with NF-L-rod (amino acids 77–364), as assessed by β-galactosidase assays (left) and Ura selection (middle) **[AU: OK?]**. NUDEL-CC did not interact with NF-L-rod. Single transformation of yeast with NUDEL-CC, NUDEL-FL or NF-L-rod plasmids did not produce interactions. A schematic representation (right) illustrates the simplified primary structures of NF-L and NUDEL proteins.

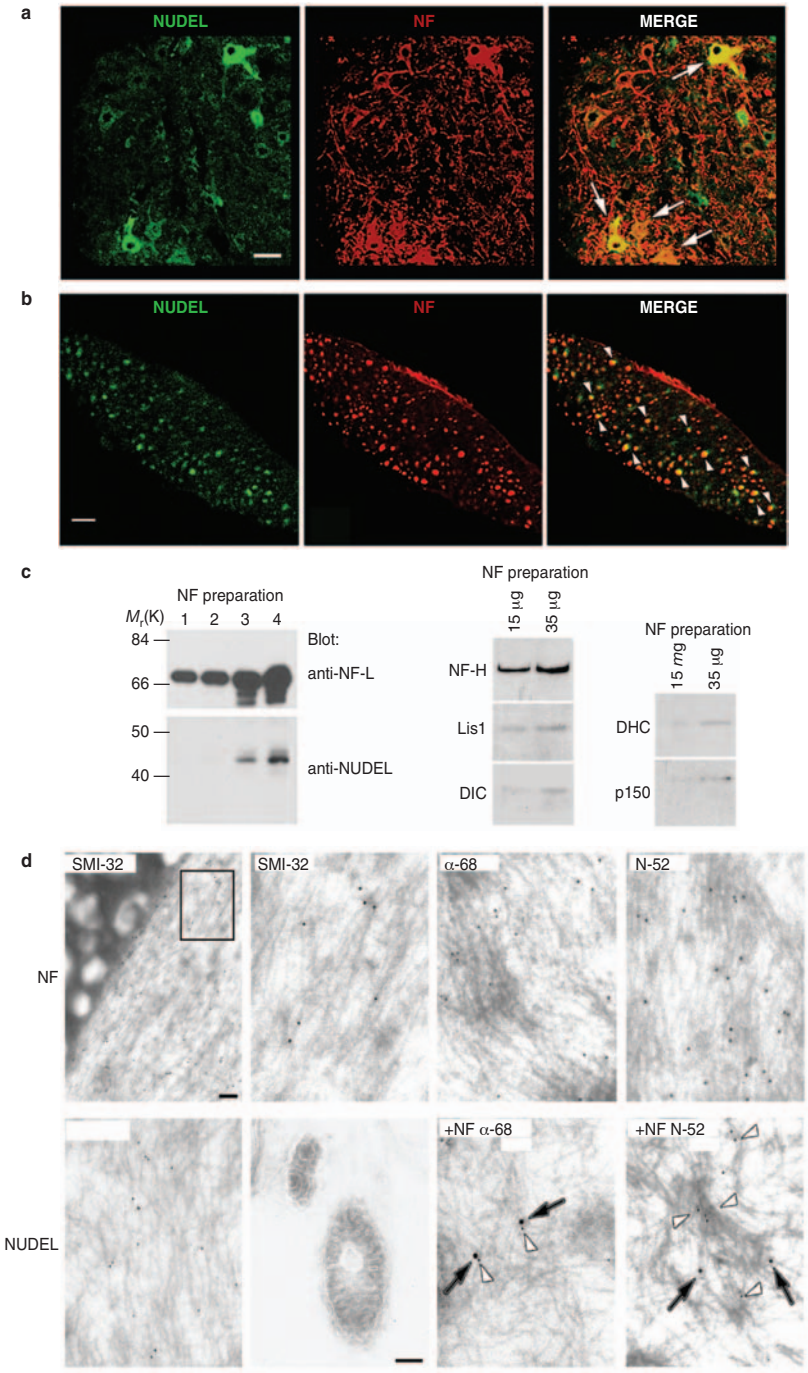

Figure 2 NUDEL associates with NF structures *in vivo*. (**a**) Confocal microscopy images of double-immunofluorescence staining for NUDEL and NF in the ventral horn of a wild-type spinal cord. A moderate-to-intense co-localization of NUDEL and NF-L was detected in motor neuron cell bodies, the primary site for NF assembly, and in neuronal processes (white arrows). Scale bar represents 30 μm. The following antibodies were used: anti-NF-L (NR-4, α-68, AB1983) and anti-NUDEL (210, 211). (**b**) Confocal microscopy images of double-immunofluorescence staining for NUDEL and NF in spinal motor neurons from the ventral root of a wild-type spinal cord. A moderate-to-intense co-localization of NUDEL and NF proteins (SMI-33) is detected in motor axons (white arrows). Scale bar represents 20 μm. (**c**) NUDEL co-purified with NF proteins in preparations containing 35 (lane 4) and 50 μg (lane 5) **[AU: lane 5 seems to be absent, please clarify]** of purified NF. NUDEL levels were undetectable in preparations containing 15 μg of NFs under light film exposure (lanes 1 and 2). The NUDEL-associated protein Lis1 and components of the retrograde transport machinery (DIC), dynein heavy chain (DHC) and p150) were also detected in NF preparations containing 35 μg of proteins, consistent with previous findings[18]. (**d**) Single- and double-immunogold-labelling of spinal motor axons with NF and NUDEL antibodies. Top panels show staining of NFs with antibodies specific to NF-L or NF-H (α-68, SMI-32, N-52). Enlargement of the top left panel is shown in the adjacent panel. NUDEL was found on NF structures, but not on mitochondria in motor axons (bottom panels). Consistent with this, NUDEL was detected in close proximity to the NF structure, as assessed by double-immunogold labelling with two different sizes of gold particles (5 nm for NF and 15 nm for NUDEL; bottom). Four animals (12–23 motor axons from each) were analysed. All scale bars represent 100 nm. **[AU: please say what the arrows indicate]**

(GST) or GST–NUDEL fusion proteins. Both NF-L and NF-H proteins were pulled down by GST–NUDEL, but not by GST (Fig. 1a). In contrast, GST–NUDEL did not pull-down NF-M. Lis1, which was much more abundant in the soluble fraction, was also efficiently pulled down by GST–NUDEL, but not by GST (Fig. 1a). These results suggest that NUDEL can form soluble complexes with NF-L and NF-H proteins in the adult mouse CNS. In addition, NUDEL co-immunoprecipitated with both NF-L and NF-H from the soluble fraction of brain lysates (Fig. 1b). Together, these data strongly support the idea that NUDEL associates with soluble NF-L and NF-H proteins.

To determine whether NUDEL and NF subunits interact directly, NF triplet was purified from mouse spinal cords[24] and far-western overlays were performed. Incubation of purified NFs fractionated on membranes with GST–NUDEL highlighted specific binding of NUDEL to NF-L, but not to NF-M or NF-H proteins, as detected by GST and NUDEL antibodies (Fig. 1c). This specific binding occurred in a dose-dependent manner, as increasing the levels of NF-L (from 15 to 50 μg) resulted in stronger signals with all three antibodies. The absence of immunoreactivity in NF preparations from NF-L knockout animals confirmed that NUDEL binds specifically to NF-L (Fig. 1c). Similarly, the His–NUDEL fusion protein also bound to NF-L in the overlay assays (Fig. 1d). These observations indicate that NUDEL interacts directly with NF-L, but not with NF-H, although it can form soluble complexes with NF-H. [**AU: OK?**]

The yeast two-hybrid system was used to map the interaction domains between NUDEL and NF-L. Both full-length (amino acids 1–345) and carboxy-terminal (amino acids 191–345) NUDEL proteins interacted with the rod domain of NF-L (amino acids 77–364; which contains two coiled-coil sub-domains), as identified by β-galacatosidase assays and Ura-3 counter-selection (Fig. 1e). In contrast, the coiled-coil domain of NUDEL (NUDEL-CC; amino acids 1–174) did not interact with the rod domain of NF-L. These results indicate that the C terminus of NUDEL is sufficient for a direct interaction with the NF-L rod.

Next, the *in situ* localization of NUDEL–NF complexes was determined in cortical neurons and spinal motor neurons. Confocal microscopy demonstrated that both NUDEL and NF-L were present in neuronal cell bodies (Figs 2a and 5b). This compartment is enriched with NF subunits and constitutes the primary subcellular site for NF assembly. Collectively, our results indicate a direct NUDEL–NF-L interaction and an indirect NUDEL–NF-H association in the soluble fraction of the adult mouse CNS.

NUDEL associates with neurofilament structures *in vivo*

Interestingly, NUDEL was also detected in neuronal processes, including motor axons of ventral root from lumbar spinal cords and elongating axons of cortical neurons (Fig. 2a, b; also see Supplementary Information, Fig. S3c). Furthermore, NUDEL co-purified with NF proteins in axonal NF preparations from spinal cords (Fig. 2c), suggesting an association with filaments *in vivo*. Immunogold-electron microscopy with spinal motor axons provided further evidence for an *in vivo* association between NUDEL and NF structures. NF antibodies conjugated to gold particles adorned typical NF structures (Fig. 2d, top). NUDEL antibodies conjugated to gold particles also decorated the NF structures, but were absent from intra-axonal structures such as mitochondria and myelin (Fig. 2d, bottom two left-hand panels; also see Supplementary Information, Fig. S1). Double-immunogold labelling with two different sizes of gold particle highlighted the close proximity of NUDEL and NFs (Fig. 2d, bottom two right-hand panels). Thus, NUDEL not only interacts with NF subunits in the soluble fraction, but also associates with polymerized NF structures in neuronal processes. Together, these results provide evidence for an *in vivo* association between NUDEL and NFs in neurons.

NUDEL facilitates NF polymerization but does not form polymers with NF proteins

As NUDEL binds directly to soluble NF-L through the rod domain, we reasoned that NUDEL may function in the assembly of NFs. Highly purified, unassembled, NF proteins from bovine spinal cord were polymerized under assembly conditions. Notably, incubation of full-length His–NUDEL with NF subunits facilitated the assembly of NFs over a period of 30 min, as determined by turbidity assays (A_{350}; Fig 3d, left) and electron microscopy (Fig. 3a, right). In contrast, minimal NF polymerization occurred when NFs were incubated alone or with NUDEL-CC, which does not bind NF-L (Fig. 3a). To further verify the role of NUDEL in NF assembly, we took advantage of the known chymotrypsin digestion pattern of NF proteins after polymerization. The cleavage of NF-L subunits by the protease preferentially yielded a fragment with a relative molecular mass (M_r) of 40,000–45,000, which consists of part of the rod domain (NF-L-rod)[24,25]. This cleavage is prevented by NF polymerization, which requires rod–rod interactions[24,25]. Assembly preparations containing NFs alone, or NFs with NUDEL-CC, [**AU: OK?**] exhibited a similar NF-L/NF-L-rod ratio (approximately 1) after digestion (Fig. 3b). A higher NF-L/NF-L-rod ratio (approximately 2) was observed in assembly preparations containing NUDEL-FL, suggesting a higher degree of polymerization. Together, these observations demonstrate that NUDEL facilitates the assembly of NFs *in vitro*.

To further assess the role of NUDEL in NF polymerization, NF and NUDEL cDNAs were transfected into SW13-vimentin$^-$ cells, a human adrenal-carcinoma-derived cell line that does not express any endogenous cytoplasmic intermediate filaments[26]. NFs are obligate heteropolymers *in vivo*, containing NF-L and either NF-M or NF-H[13,27]. As expected, a NF network composed of assembled NF proteins formed after the double-transfection of SW13$^-$ cells with NF-L and NF-H (Fig. 3c, top left; ref. 26). In contrast, cells transfected with NUDEL and NF-L, or NUDEL and NF-H, did not exhibit a filamentous network, although NUDEL occupied overlapping compartments with NF-L and NF-H proteins (Fig. 3c, top right and bottom left). In cells that were triple-transfected with NUDEL, NF-L and NF-H, NUDEL again did not assemble with filaments (Fig. 3c, bottom right). These findings indicate that NUDEL does not form polymers with NF proteins. These observations are consistent with the predicted structure of NUDEL, which lacks the rod domain that is necessary for the polymerization of intermediate filaments.[**AU: OK?**]

Depletion of *NUDEL* in a neuroblastoma cell line by RNAi causes NF abnormalities that impact on NF assembly and cell integrity [AU: Please shorten Title to fit on one line.]

To examine the role of NUDEL on NFs, *NUDEL* expression was knocked down by RNAi. In the neuroblastoma CAD cells transfected with *NUDEL* RNAi, endogenous NUDEL protein was diminished by 50% as identified by western blot analysis (Fig. 4a). No decrease was observed in CAD cells transfected with a control plasmid encoding a random sequence that has no homology to any known messenger RNA (mRNA). Notably, the levels of NF-L decreased concomitantly with those of NUDEL after targeting of *NUDEL* by RNAi. In contrast, the levels of other NUDEL binding partners such as the dynactin subunit p150, dynein intermediate chain, as well as other cytoskeletal components (such as actin, α-Tubulin and Lis1), remained unchanged (Fig. 4a). Thus, the reduction of NUDEL imposed a specific effect on NF-L levels.

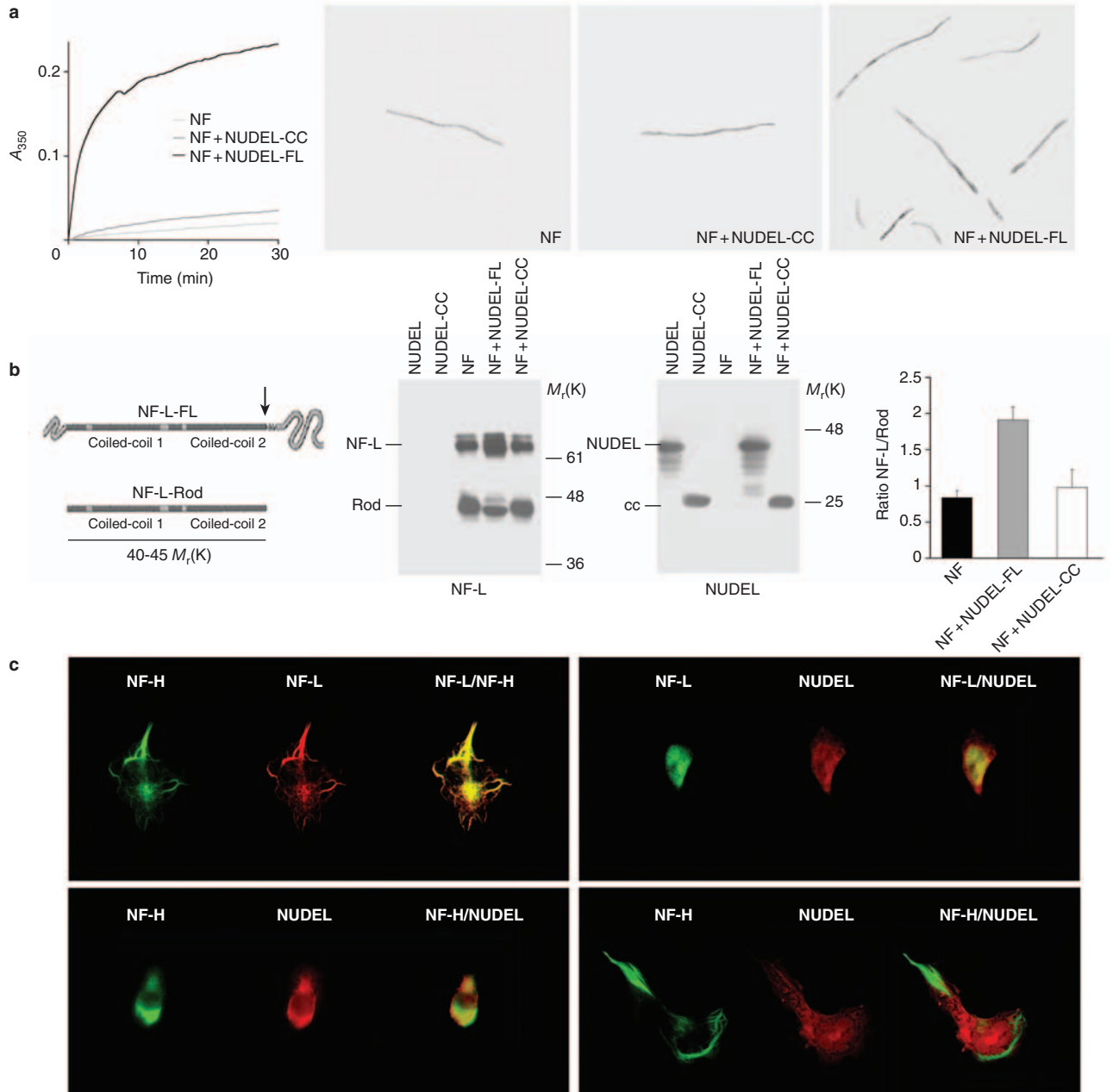

Figure 3 NUDEL facilitates NF polymerization *in vitro*, but does not form polymers with NF proteins. (**a**) Incubation of NUDEL-FL with purified NF proteins in assembly conditions favours the polymerization of NFs as detected by increased turbidity (A_{350}). Conversely, NUDEL-CC (which does not bind NF-L) had no significant affect on turbidity. Electron microscopy demonstrated that more filaments can be detected in assembled NF preparations containing NUDEL-FL when compared to preparations with NFs alone and NF plus NUDEL-CC. **[AU: please indicate what the time points refer to]** (**b**) Chymotryptic digestion of polymerized oligomers and filaments in the presence of NUDEL-FL demonstrates a higher NF-L/rod ratio (up to twofold greater), when compared to ratios derived from assembled NF preparations with or without NUDEL-CC. A high NF-L/rod ratio indicates protection of rod–rod interactions and thus higher polymerization. Chymotrypsin had little effect on NUDEL and NUDEL-CC. (**c**) Assembly assays of NUDEL with NFs in SW13$^-$ cells indicated that NUDEL does not assemble with NFs. NUDEL is unable to form a filamentous network with either NF-L or NF-H (top right and bottom left) in contrast to the co-assembly of NF-L and NF-H (top left). In the triple-transfected cells (NUDEL, NF-L and NF-H), a network was formed by NF-L and NF-H, but NUDEL was unable to assemble into this network (bottom right). Scale bar represents 15 μm.

As NF-L is the key NF assembly subunit, we investigated the consequence of decreased NUDEL levels on the formation of NF networks in CAD cells by using a NF-M–GFP plasmid as a marker for NF assembly (see Supplementary Information, Fig. S2). NF-M–GFP filaments were distributed in the processes of CAD cells double-transfected with NF-M–GFP/control plasmids (Fig. 4b, second row). In NF-M–GFP/*NUDEL*-RNAi double-transfected cells, however, NF-M–GFP accumulated in the cell body and processes, and formed multiple spheroid-like aggregations characteristic of altered NF assembly (Fig. 4b, top row, white arrowheads and second row). Electron microscopy

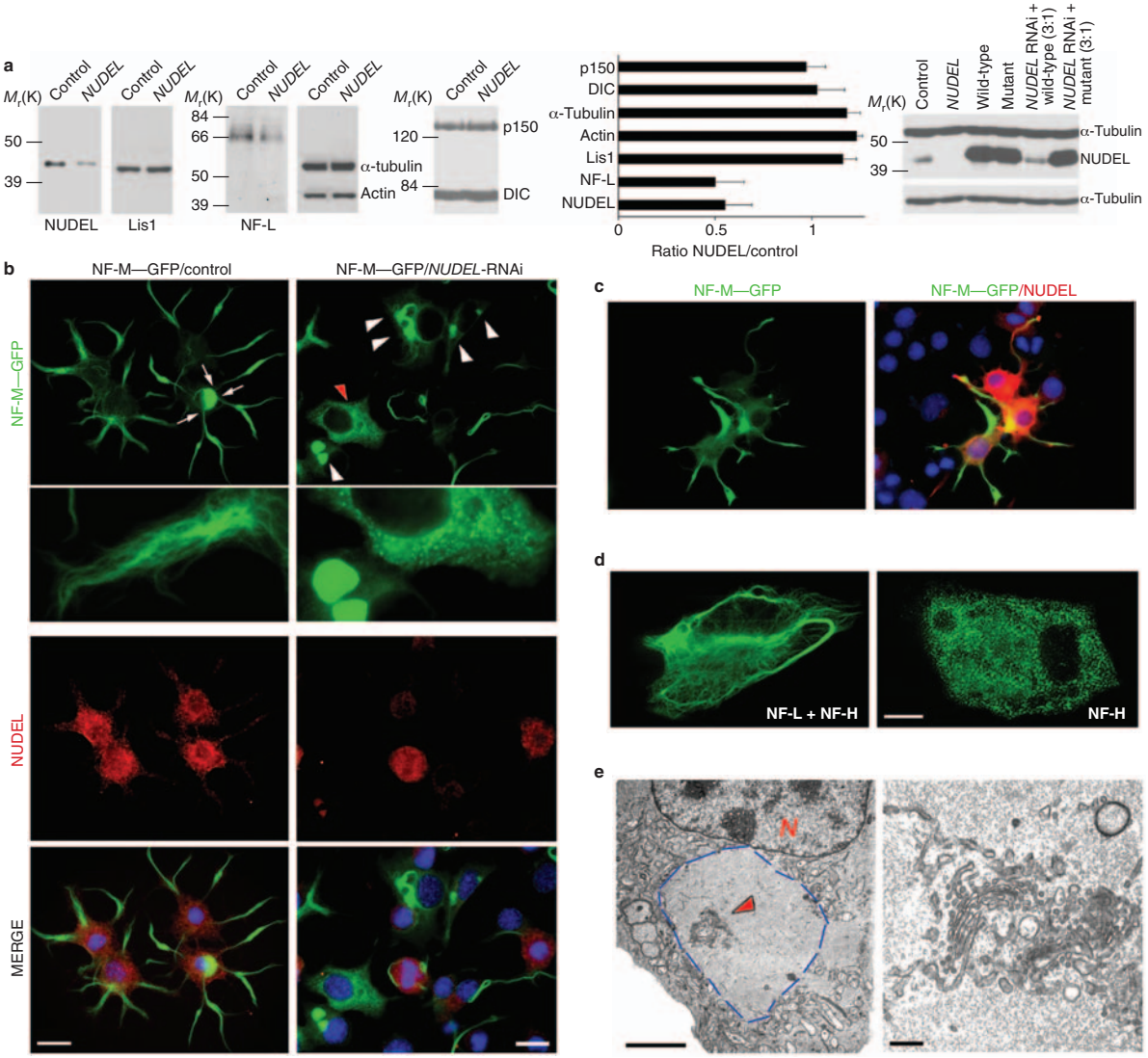

Figure 4 Silencing expression of *NUDEL* in CAD cells by RNAi causes cytoskeletal NF abnormalities and loss of neuronal integrity. **[AU: Please shorten Title to fit on one line.]** (**a**) Western blot analysis of lysates from differentiated neuroblastoma CAD cells transfected with *NUDEL*-RNAi sequence or with an unrelated RNAi control sequence. The specificity of NUDEL RNAi was demonstrated after co-transfection of *NUDEL*-RNAi plasmids and plasmids expressing either wild-type *NUDEL* or an RNAi-resistant *NUDEL* mutant cDNA containing several silent mutations that cannot be targeted by *NUDEL*-RNAi. Although *NUDEL*-RNAi efficiently knocked down wild-type NUDEL, expression of the mutant NUDEL was not suppressed by the same plasmid, providing evidence that *NUDEL*-RNAi is specific in knocking down endogenous NUDEL. The down-regulation of endogenous NUDEL is associated with a specific decrease of NF-L but does not affect the levels of molecular motor components, such as, p150, Lis1, DIC and cytoskeletal proteins (such as α-Tubulin and actin). Transfections and western blot analysis were performed in triplicate. (**b**) Immunofluorescence microscopy staining of differentiated CAD cells double-transfected with NF-M–GFP, and control or *NUDEL*-RNAi vectors. Differentiated CAD cells double-transfected with *NUDEL*-RNAi and NF-M–GFP plasmids accumulate NF-M protein in cell bodies (white arrowheads). Approximately 38% (487/1317) of cells with decreased NUDEL levels showed these NF accumulations, whereas only 5% (26/533) of control cells showed such accumulations. The red arrowhead points to a cell transfected with *NUDEL*-RNAi and NF-M–GFP that has a punctate staining characteristic of completely unassembled NF-M protein **[AU: please say what the enlarged panels represent, and also say how much the increase in magnification is]**. In contrast, differentiated CAD cells double-transfected with control and NF-M–GFP plasmids produced a neurofilamentous network of processes. In many cells, a thin filament is often seen radiating from a region close to the nucleus (white arrows). Scale bars represent 30 μm (left) and 40 μm (right). The NUDEL antibodies used were 210 and 211; nuclei were stained with DAPI (blue). (**c**) Low level expression of RNAi-resistant-NUDEL-protein containing several silent mutations rescued the cellular distribution of NFs in the presence of *NUDEL*-RNAi. Left, NF-M–GFP alone; right, NF-M–GFP and NUDEL. Nuclei were stained with DAPI (blue). **[AU: OK?]** (**d**) NF-L and NF-H proteins formed a filamentous network in SW13^{-} cells, a cell line lacking intermediate filaments. In the absence of NF-L, NF-H produced a puntacte immunofluorescence staining pattern typical of unassembled NF proteins. This phenotype was indistinguishable from that observed in some CAD cells transfected with the *NUDEL*-RNAi. Scale bar represents 10 μm. (**e**) Electron microscopy of NF accumulations in cells transfected with *NUDEL*-RNAi and NF-M–GFP. Accumulations of NFs close to the nucleus were observed in NF-M–GFP/*NUDEL*-RNAi cells (blue lines). Left, organelles such as the Golgi apparatus could be found in the inclusions (red arrowheads). Right, a fraction of fragmented Golgi in an inclusion. Scale bar represents 30 μm (left) and 300 nm (right).

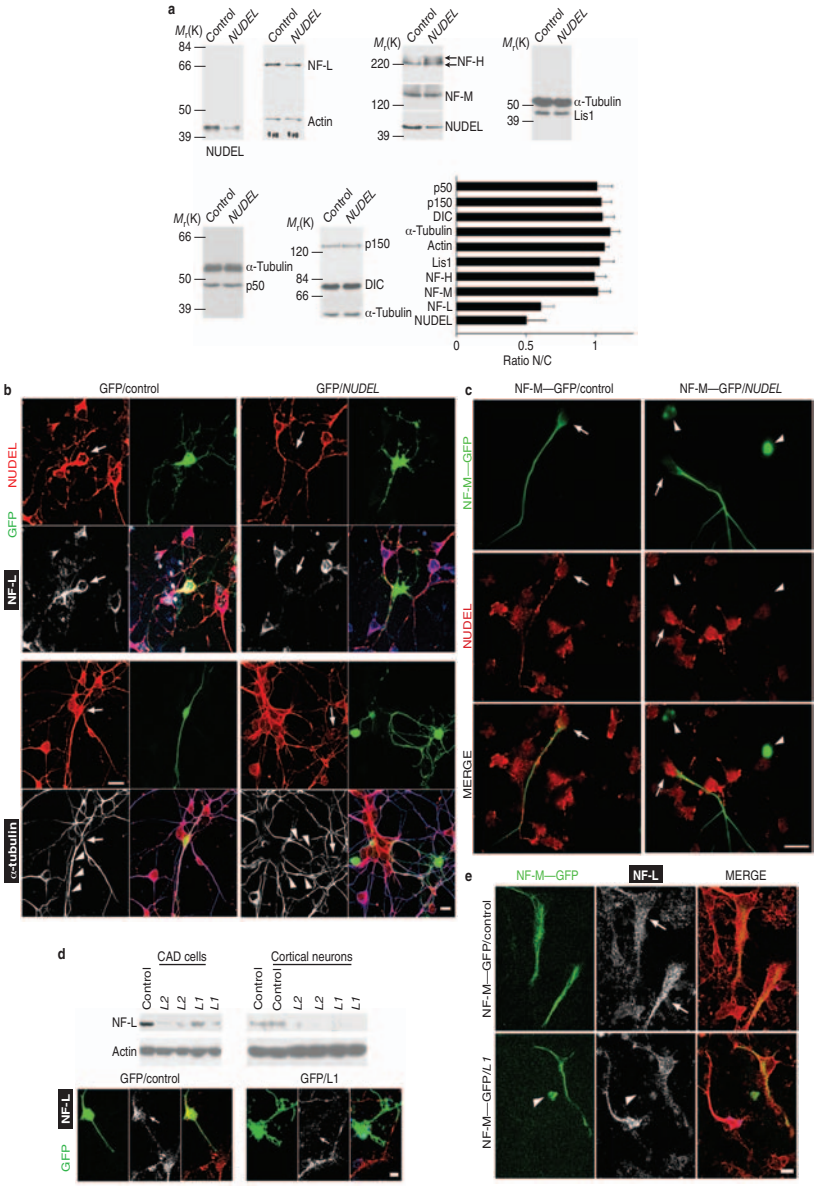

Figure 5 Genetic knockdown of NUDEL in primary cortical neurons disrupts NF homeostasis and causes cell shape abnormalities similarly to *NF-L*-RNAi. **[AU: Please shorten Title to fit on one line.]** (**a**) Western blot analysis of lysates from cortical neurons electroporated with *NUDEL*-RNAi or with an unrelated RNAi control sequence. A 60% decrease in NUDEL levels was observed in cortical cultures of neurons electroporated with *NUDEL*-RNAi for a concomitant 40% decrease in NF-L in the same cultures. Levels of p50, p150, Lis1, DIC and cytoskeletal proteins (such as NF-M, NF-H, α-Tubulin and actin) remain unchanged. Note that NF-H becomes hyperphosphorylated. Five different electroporations were performed and western blot analysis was performed in triplicate. (**b**) Confocal immunofluorescence microscopy images of cortical neurons transfected with GFP/*NUDEL*-RNAi (top right) or GFP/control (top left), and stained with NUDEL (red) and NF-L (white). GFP neurons transfected with *NUDEL*-RNAi (82/85) demonstrated a concomitant down-regulation in levels of NUDEL and NF-L associated with a fragmented irregular GFP staining. The same decrease and morphology was not observed in neurons transfected with both GFP and the control plasmid ($n = 44$). White arrows point to transfected neurons. Neuronal processes in GFP/*NUDEL*-RNAi-transfected neurons were not completely lost, as determined by α-Tubulin staining (white). The primary antibodies used were as follows: anti-NF-L (NR-4), anti-NUDEL (210, 211) and anti-α-Tubulin. Scale bar represents 10 μm. (**c**) NF accumulations in NF-M–GFP/*NUDEL*-RNAi-electroporated neurons. NF-M–GFP assembled and localized in axons of NF-M–GFP/control-transfected cells (left, white arrows), whereas it accumulated exclusively in neurons co-electroporated with NF-M–GFP/*NUDEL*-RNAi (right) that exhibit a decrease of NUDEL. The majority of NF-M–GFP/*NUDEL*-RNAi neurons (65%; 241/367) demonstrated NF-M–GFP accumulations, whereas only 11% (33/298) of NF-M–GFP/control neurons had this feature. Scale bar represents 15 μm. (**d**) *NF-L*-RNAi plasmids L1 and L2 efficiently knocked down NF-L expressed ectopically in CAD cells. These plasmids also reduced the levels of endogenous NF-L in primary cortical neurons, as demonstrated by western blot analysis and confocal immunofluorescence microscopy for L1. A known effective sequence was used as a positive control for L2, (ref. 29). The cell-shape abnormalities in the GFP/*L1*-transfected neurons were reminiscent of those caused by the *NUDEL*-RNAi (right). Scale bar represents 50 μm. (**e**) NF accumulations in NF-M–GFP/L1-electroporated neurons. Confocal immunofluorescence microscopy images of cortical neurons transfected with NF-M–GFP/control (top) or NF-M–GFP/*L1* (bottom) and stained for NF-L. NF-M–GFP localized in processes in NF-M–GFP/control cells (white arrows), whereas it accumulated exclusively in neurons co-electroporated with NF-M–GFP/L1 that exhibit a decrease of NF-L (white arrowheads). These accumulations were reminiscent of those found in *NUDEL*-RNAi-transfected cells and NF-L-null neurons[13,25,32]. Scale bar represents 10 μm.

demonstrated that NF accumulations in the cell body contained organelles such as mitochondria and fragmented membranes from the Golgi apparatus (Fig. 4e, red arrowhead). This is reminiscent of the disintegration of the Golgi apparatus observed in degenerating neurons with NF abnormalities[28]. At a cellular level, these NF accumulations can be alleviated by low-level of expression of an RNAi-resistant NUDEL mutant (Fig. 4c).

Previous studies have shown that a partial decrease of NF-L causes accumulation of NFs, whereas a complete down-regulation of NF-L produces a punctate pattern of NF-M and NF-H, which is characteristic of completely unassembled NF subunits[25,26,29]. Notably, some NF-M–GFP/*NUDEL*-RNAi-transfected cells demonstrated a punctate NF-M–GFP distribution, which is possibly the result of a complete destabilization of NF-L (Fig. 4b, red arrowhead and second row). In support of this view, transfection of NF-M or NF-H into a cell line devoid of NF-L produced an identical NF punctate pattern that was indistinguishable from a number of CAD cells transfected with the *NUDEL* RNAi (Fig. 4d). In addition, an increased ratio of soluble (non-assembled) versus insoluble (assembled) NFs, and abnormal phosphorylation of NF-H (features of disrupted NF assembly) were detected in lysates from cells transfected with *NUDEL* RNAi (see Supplementary Information, Fig. 2c–d). Together, these results provide evidence that NUDEL functions in NF assembly *in vivo*. [**AU: OK?**]

Loss of NUDEL in primary cortical neurons alters neuronal processes

As assembled NFs are important for the stability of neuronal processes, we questioned this paradigm after the depletion of NUDEL in primary cortical neurons. Addition of *NUDEL* RNAi selectively knocked down NUDEL and NF-L by 50% in electroporated primary cortical neurons (Fig. 5a). It should be noted that in *NUDEL*-RNAi-treated cells, NF-H became hyper-phosphorylated. Whereas levels of p50, p150, Dynein intermediate chain (DIC), Lis1, NF-M, NF-H, actin and α-Tubulin remained stable (Fig. 5a). The decrease in levels of NF-L by *NUDEL*-RNAi was not the result of a decrease in NF-L transcription, as mRNA expression was unaltered (see Supplementary Information, Fig. 3b).

Consistent with western blot analysis, individual neurons co-transfected with *NUDEL*-RNAi and GFP demonstrated a selective decrease of NF-L that paralleled the decrease of NUDEL, as identified by confocal microscopy (Fig. 5b, white arrows; also see Supplementary Information, Fig. S3a). Notably, these neurons exhibited a varicose-like irregular GFP staining, suggesting a destabilization of processes and cell-shape abnormalities. However, the processes were not completely lost, as indicated by α-Tubulin staining (Fig. 5b, white arrowheads). In contrast, neither morphology, nor NUDEL and NF-L levels, were altered in neurons co-transfected with the control and GFP plasmids.

Evidence that NUDEL is important for axonal NFs came from co-electroporation of NF-M–GFP and *NUDEL*-RNAi plasmids in primary cortical neurons. A distribution of NF-M in neuronal processes was observed in neurons double-electroporated with NF-M–GFP/control plasmids (Fig. 5c; also see Supplementary Information, Fig. S3a). In contrast, neurons electroporated with NF-M–GFP/*NUDEL*-RNAi demonstrated a decrease in NUDEL and accumulated NFs, (Fig.5c, arrowheads) [**AU: OK?**] which may impede the formation of axonal NF-M–GFP.

The varicose-like irregular cell-shape and NF-M–GFP accumulations caused by *NUDEL*-RNAi were not artefacts, but most probably resulted from the destabilization of NF-L. Indeed, knockdown of NF-L by two different *NF-L*-RNAi plasmids [**AU: OK?**] recapitulated these phenotypes in neurons (Fig. 5d, e). These results indicate that NF-L may be the target of *NUDEL* RNAi. These data also suggest that through the stabilization of NF-L rod domain, NUDEL is required for the assembly and transport of NFs in axons, as well as for their maintenance.

Silencing the expression of NUDEL in the post-natal mouse brain by RNAi causes NF alterations reminiscent of neurodegeneration [AU: Please shorten Title to fit on one line.]

To determine whether NUDEL is important for NF homeostasis *in vivo*, *NUDEL*-RNAi and GFP were co-expressed in E15/17 mouse brains by *in utero* electroporation[30]. The brains were analysed before post-natal days four and eight to ensure that the brain reached maturity and expressed NF proteins. These times were chosen because expression of both NUDEL and NF proteins peaks during early post-natal days[11,12]. As shown by confocal miscroscopy, non-transfected neurons in the cortex exhibited NF staining in close proximity to the axon hillock and in processes; this corresponds to the normal distribution of NFs and is similar to the pattern observed in cultured neurons (Fig. 6a, white arrowheads). In contrast, GFP-positive neurons demonstrated either accumulation of NFs close to the nucleus or decreased levels of NF-L, or both (Fig. 6a, b, white arrows). Note that NF accumulations bent the nucleus of neurons and induced nuclear fragmentation in 50% (17/32) of cells (Fig. 6a, asterisk; also see Supplementary Information, Fig. S4). A high-resolution confocal microscopy image demonstrated a diffuse accumulation of NFs in the cell bodies of electroporated neurons (Fig. 6b). This phenotype was suppressed by expression of the RNAi-resistant *NUDEL* cDNA (Fig. 6c, white arrowhead), thereby providing further evidence of specificity. These findings indicate that NUDEL impacts on the homeostasis of NFs and neuronal integrity *in vivo*.

Downregulation of NUDEL coincides with NF abnormalities in a mouse model of neurodegeneration

As NUDEL is important for NF assembly and neuronal integrity *in vivo*, we reasoned that variations in levels of NUDEL may coincide with NF defects in a mouse model of neurodegeneration. We analysed transgenic mice overexpressing a mutant form of superoxide dismutase 1 ($SOD1^{G37R}$), which is implicated in amyotrophic lateral sclerosis (ALS; the most common form of human motor neuron disease)[31]. These mice exhibit a loss of neuronal processes and motor neuron degeneration that is reminiscent of ALS[31]. Notably, reduced NUDEL levels were observed in fractionated lysates of young presymptomatic mutant *SOD1* mice, as identified by a decrease in NUDEL/actin and NUDEL/p150 dynactin subunit ratios (Fig. 7a). A decrease in NUDEL levels was also observed in individual motor neurons (Fig. 7b). In these mice, the distribution of NF-L also markedly changed in the young SOD1 mice, suggesting abnormalities in the homeostasis of NF proteins (Fig. 7a). Moreover, there is a loss of higher-molecular-weight NF-L–NF-H complexes in these animals, further indicating alterations in NF stochiometry and assembly (fractions 10–12). In older ALS mice (9–12 months old), a marked decrease in NUDEL and NF-L was observed, whereas levels of other cytoskeletal or motor-related molecules remained stable (Fig. 7c; also see Supplementary Information, Fig. S5a). Down-regulation of NUDEL was associated with cytoskeletal NF abnormalities over the course of the disease (see Supplementary Information, Fig. S5b).

In addition to these alterations, the association of NF-H with NUDEL or p50–p150 complexes was lost in mutant SOD1 animals, as determined by co-immunoprecipitation experiments (Fig. 7d). The p50–p150 complex was, however, preserved in these mice, indicating that NF alterations might be independent of the dynein/dynactin transport complex. Finally, overexpression of human NF-H protein, which

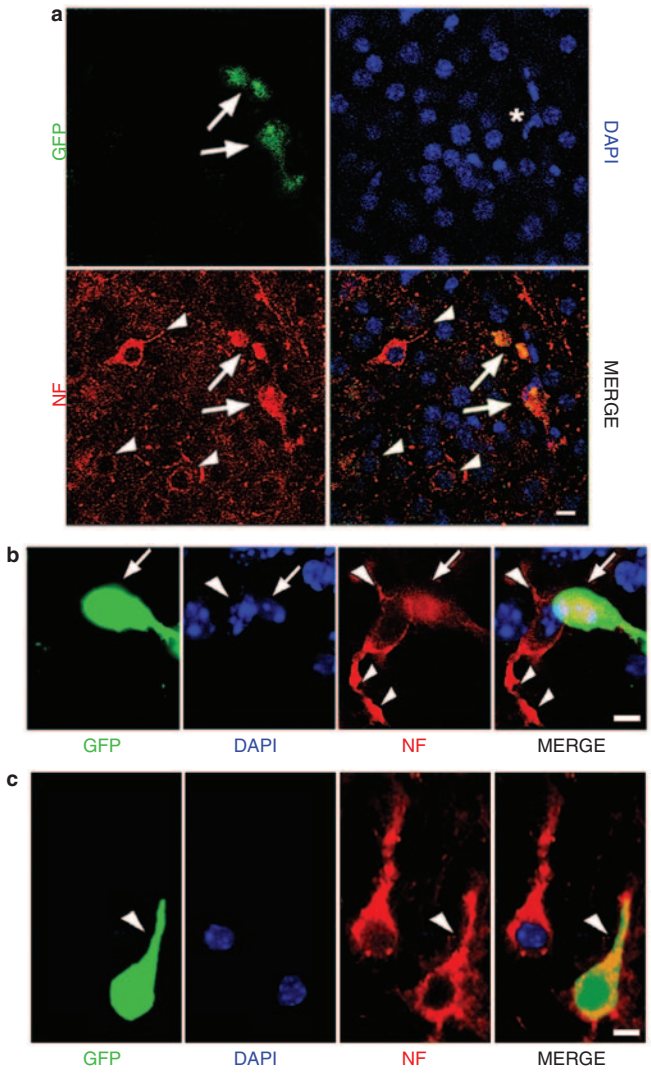

Figure 6 Genetic knockdown of NUDEL in the post-natal mouse brain disrupts NF homeostasis in a manner reminiscent of neurodegeneration. **[AU: Please shorten Title to fit on one line.]** (**a**) **[AU: diagram has been removed as it doesn't seem entirely necessary and space is extremely limited]** Embryonic mouse brains were electroporated *in utero* with *NUDEL*-RNAi/GFP at day 15/17 (E15/17) and analysed at post-natal day 4/8 (P4/P8). GFP/*NUDEL*-RNAi-electroporated neurons showed accumulations of NF-H (N-52; red) in the cell bodies of neurons (white arrows). Bending and fragmentation of the nucleus (asterisk) was observed in 17/32 of cells with these accumulations. GFP-negative neurons showed a normal NF staining pattern in the cell body, close to the axon hillock and also in the main process (white arrows). Four different animals were analysed (60 neurons in total). Nuclei were stained with DAPI (blue). Scale bar represents 10 μm. (**b**) A high-resolution image depicts the diffuse reduction and accumulation of NF-L (α-68) in the cell bodies of electroporated neurons (white arrow), whereas non-electroporated neurons showed normal NF staining in the cell body and main process (white arrowheads). Nuclei were stained with DAPI (blue). Scale bar represents 10 μm. (**c**) NF abnormalities caused by *NUDEL*-RNAi in neurons were suppressed by the expression of RNAi-resistant NUDEL protein (white arrowhead). Nuclei were stained with DAPI (blue). Scale bar represents 10 μm.

confers protection to motor neurons against mutant SOD1 toxicity[32,33], prevented the decrease of NUDEL in this background (Fig. 7d; also see Supplementary Information, Fig. S5c). These observations support the hypothesis that down-regulation of NUDEL is associated with NF defects and a loss of neuronal integrity during disease progression.

DISCUSSION

During development, NUDEL is thought to function in neuronal migration, corticogenesis and neurite outgrowth. However, the role of NUDEL in the adult CNS is less clear. Similarly, the mechanisms promoting the assembly of NF subunits into polymers/filaments also remains unclear. Here, we provide evidence that NUDEL associates with soluble pools of NF-L and NF-H subunits, as well as with NF structures. Through these associations, NUDEL impacts on the assembly and homeostasis of the neurofilamentous network. These functions have direct repercussions for the architecture and integrity of neurons *in vivo*, and may be involved in neurodegeneration featuring NF defects.

NUDEL exists in soluble complexes with NF-L and NF-H proteins in the adult CNS. The C-terminal half of NUDEL binds directly to the rod domain of the NF-L subunit, whereas the association of NUDEL and NF-H is indirect (Figs 1, 7). Importantly, NUDEL facilitates the *in vitro* polymerization of NFs, but does not assemble with NF proteins (Fig. 3). Furthermore, knockdown of *NUDEL* by RNAi in CAD cells, primary cortical neurons and post-natal mouse brain, specifically depletes NF-L at the protein level and results in phenotypes similar to those observed in both cell lines and mice that partially or completely lack NF-L. Indeed, genetic knockdown of NUDEL disrupts NF stoichiometry, which, in turn, results in impaired NF assembly and transport, accumulation of NFs and changes in neuronal morphology (Figs 4–6; also see Supplementary Information, Figs S2, S3). These phenotypes are very similar to those observed after knockdown of *NF-L* by RNAi. On the basis of these observations, we propose that NUDEL stabilizes NF-L at the rod-domain, thereby favouring polymerization of NFs under appropriate assembly conditions (Fig. 8). In this model, binding of NUDEL to NF-L may expose the NF-L rod-domain in a conformation that is distinct from the one observed in polymeric rod–rod interactions. The direct versus indirect association of NUDEL with NF-L and NF-H, respectively, during NF assembly may be related to the intrinsic architecture of NFs. Whereas NF-L constitutes the core of the NF structure, NF-H composes the peripheral side-arms extending from the core[34,35]. The indirect interaction between NUDEL and NF-H may be mediated through dynein motors or accessory proteins, which are known to associate with both NUDEL and NFs[2,3,18].

The functions of NF subunits are not confined to the assembly of the NF network. Soluble NF proteins are most probably essential for the transport, turnover and exchange of subunits in mature networks, such as those found in large neurons. The evidence that soluble NF subunits translocate bidirectionally along intra-axonal microtubules with molecular motors such as kinesin and dyneins further supports the notion that soluble NF proteins have an important function in the homeostasis of the filamentous network[6–10]. This is also strengthened by the findings that soluble NUDEL–NF complexes co-fractionate and can be co-immunoprecipitated with the dynactin complex subunits p150 and p50 [**AU: OK?**] (Fig.7; also see Supplementary Information, Fig. S2). In addition to its association with NF subunits, NUDEL may also associate with the polymerized NF network (Fig. 2; also see Supplementary Information, Figs 1, 3c). Therefore, it is conceivable that after promoting NF assembly, a fraction of NUDEL remained bound to assembled filaments (Fig. 8). As the ability of NUDEL to associate with the NF network is similar to that of cytoplasmic dynein[18], we propose that there is efficient cooperation of NUDEL with the dynein complex and molecular motors to mediate the transport of NF subunits and filaments, and also to maintain turnover of the network. This hypothesis is consistent with the recent finding that NF

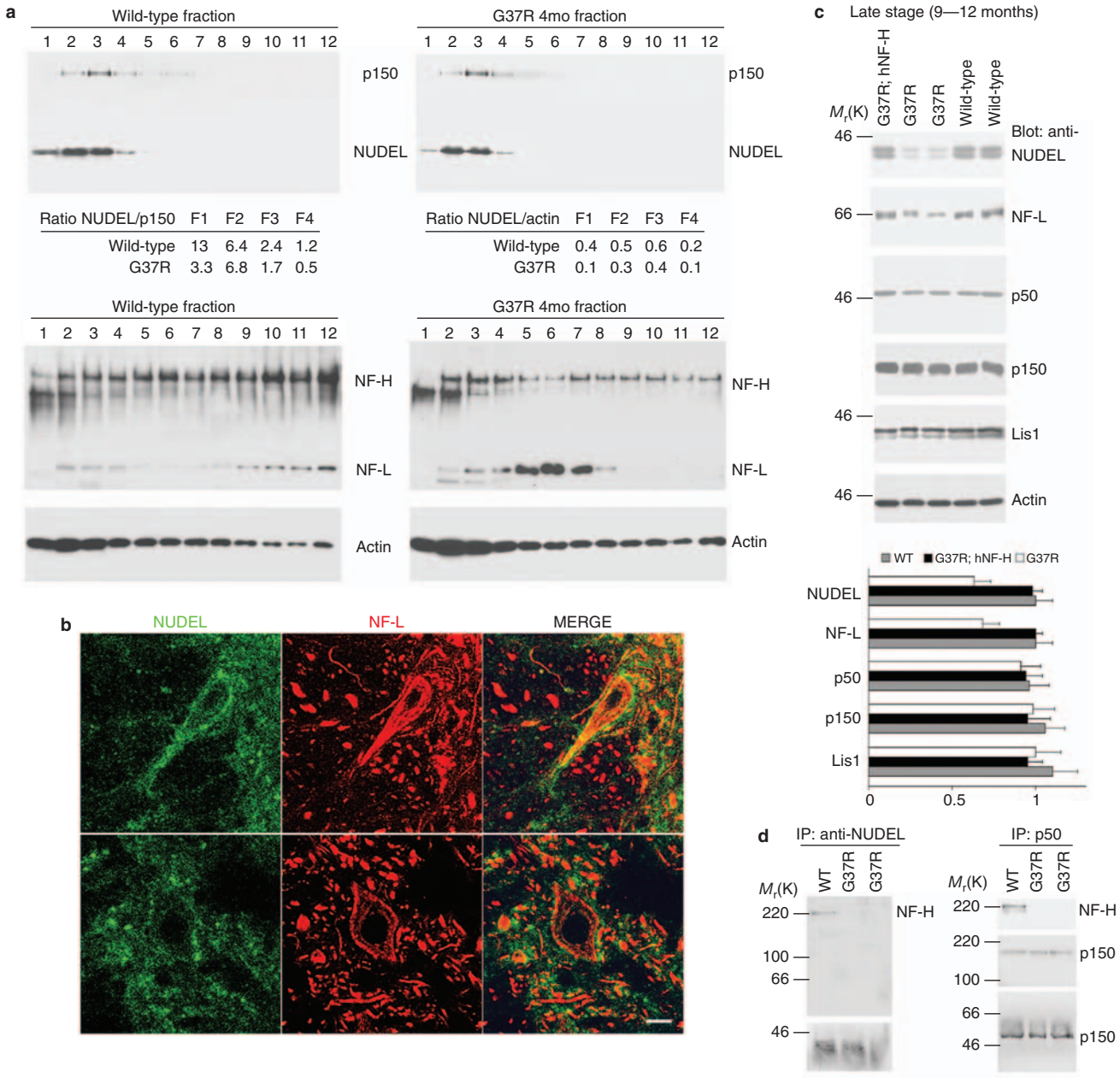

Figure 7 Downregulation of NUDEL coincides with NF defects during *in vivo* neurodegeneration. (**a**) Fractionation of NUDEL, NF-L, NF-H and p150 from spinal cord lysates of presymptomatic SOD1^{G37R} mice. In wild-type mice, NUDEL was distributed across **[AU: OK?]** low-molecular-weight fractions F1–F4 with a strong predominance in F2 and F3. In presymptomatic SOD1^{G37R} transgenic mice, NUDEL was also concentrated in F2 and F3, but levels of NUDEL were decreased in fractions F1–F4, as identified by the reduced NUDEL/p150 and NUDEL/actin ratios. The loss of high-molecular-weight NF complexes in F10–F12 and the disruption of NF-L/NF-H ratio in F5–F7 was associated with the downregulation of NUDEL in presymptomatic SOD1^{G37R} transgenic mice, suggesting altered NF assembly. Note that the distributions of actin and p150 were similar in wild-type and presymptomatic SOD1^{G37R} transgenic mice (four-month-old wild-type, $n = 3$; four-month-old SOD1^{G37R} transgenic mice (line 29), $n = 3$). The following antibodies were used: anti-NUDEL (N210), anti-NF-L (NR4), anti-NF-H (RT-97), anti-p150 and anti-actin. (**b**) A concomitant decrease in levels of NUDEL (green) and NF-L (red) was observed in individual motor neurons of SOD1^{G37R} transgenic mice (bottom), compared with wild-type (top), as detected by confocal immunofluorescence microscopy. Scale bar represents 10 μm. (**c**) Total levels of NUDEL, phospho-NUDEL, NF-L, Lis1, p150 and p50 in SOD1^{G37R} transgenic mice and wild-type littermates in the late stage of disease (9–12 months old). Only levels of NUDEL and NF-L significantly decreased in 9–12-month-old SOD1^{G37R} transgenic mice ($n = 9$). This down-regulation was prevented by the protective overexpression of hNF-H ($n = 2$). Quantification graphs show the selective destabilization of NUDEL/NF-L rescued by overexpression of hNF-H. Quantification of NUDEL levels were corrected according to levels of actin (used as a loading control). (**d**) Loss of NUDEL–NF-H, NF-H–p50–p150 interactions, but not p50–p150 interactions, in SOD1^{G37R} transgenic mice ($n = 3$). Antibodies against NUDEL or p50 pulled down NF-H from soluble fractions of wild-type mouse adult spinal cord. This association of NF-H with NUDEL or p50–p150 was disrupted in SOD1^{G37R} mice, whereas p150 still associated with p50.

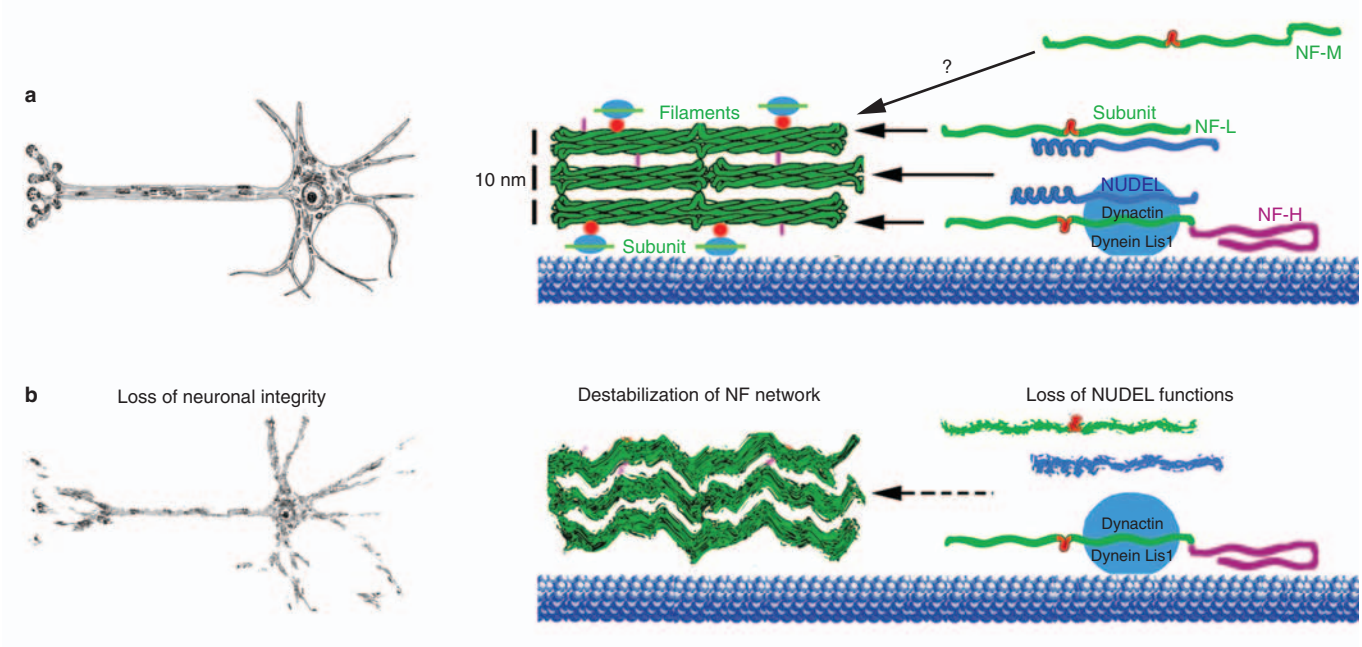

Figure 8 Roles for NUDEL in the biology of NFs and neuronal integrity. (**a**) In this model, NUDEL regulates soluble pools of NF-L (green) and NF-H (purple) proteins. NUDEL (navy) interacts directly with NF-L at the rod domain (red) **[AU: OK?]**. In parallel, NF-H is in complexes with NUDEL and the dynein/dynactin complex (sky blue). By interacting with NF-L, NUDEL favours the incorporation of NF subunits into the network during NF assembly and elongation. In conjunction with molecular motors lining the NF structures, NUDEL may also promote the transport and turnover of filaments. It is conceivable that after promoting NF assembly, a fraction of NUDEL remains bound to assembled filaments **[AU: please make clear where this is indicated]**. An unknown NF-M-binding molecule may favour loading of the subunit during NF polymerization. (**b**) Loss of NUDEL function triggers the destabilization of the NF-L key assembly subunit. **[AU: OK?]** The NUDEL–NF-H complexes are also lost. This causes a disruption of the NF stochiometry and assembly, resulting in defective axonal transport and cytoskeletal abnormalities that contribute to destabilization of neuronal processes, loss of neuronal integrity and, ultimately, to neurodegeneration. Microtubules are resized for clarity of the pictures. **[AU: 'Δ NF-L conformation [conditions for assembly]' has been deleted, as it isn't clear how this relates to the model].**

assembly is important for NF transport[36].

NFs are known to contribute to the architecture and survival of CNS neurons by stabilizing axons and dendrites. In Alzheimer's disease, Parkinson's disease and ALS, NFs are hyperphosphorylated and accumulate abnormally in neuronal perikarya and axons[6–10,37–39]. A 30–80% decrease in NF-L levels has also been reported in some Alzheimer's disease, Parkinson's disease and ALS patients[40–42]. As demonstrated here, down-regulation of NUDEL in CAD cells and primary cultured neurons results in pathological signatures associated with the destabilization of processes and fragmentation of the Golgi apparatus. Interestingly, expression of *NUDEL*-RNAi in neurons of post-natal mouse brain triggers NF abnormalities reminiscent of those observed in neurodegenerative conditions (Fig. 6). Together, these results indicate that through NF regulation, NUDEL impacts on the integrity of CNS neurons and may therefore contribute to neuronal demise. As such, downregulation of NUDEL is detected in presymptomatic $SOD1^{G37R}$ mice, a mouse model for ALS with cytoskeletal NF abnormalities (Fig. 7). As observed in neurons transfected with *NUDEL* and *NF-L*-RNAi plasmids, these mice had NF-L alterations, disrupted NF stoichiometry, and accumulations of NFs in cell bodies (Figs 4–7; also see Supplementary Information, Fig. S2), consistent with the sensitivity of NF-L to SOD1 mutants (as previously assessed by cell culture, mouse models and tissues from patients with ALS)[43,44]. The outcome of the acute down-regulation of NF-L observed in these cases most probably differs from that observed after the genetic removal of NF-L during development. In addition to NF-L alterations, a dissociation of soluble NF-H from NUDEL and p50–p150 complexes was also detected in *SOD1* mutant mice (Fig. 7d). The idea that loss of NUDEL–NF interactions contributes to this pathology is further strengthened by our analysis of the SOD1/NF-H bi-transgenic compound mice (Fig. 7c) Previous studies demonstrated that overexpression of NF-L or NF-H protects against neurodegeneration in mutant SOD1 mice[32,33,45]. As shown here, NUDEL levels are preserved in compound mice (Fig. 7c). Together, these results indicate that disruption of NUDEL functions most probably contributes to the loss of neuronal integrity and neurodegeneration.

As NUDEL knockout mice are early-embryonic lethal (as a result of apoptosis; A. Wynshaw-Boris, personal communication), [**AU: please confirm that you have the author's permission to discuss this unpublished work**] the generation of a conditional post-natal and neuron-specific knockout for NUDEL would help to further elucidate the function of the protein in the adult CNS. Future studies of mammalian homologues of the Nud family should provide exciting discoveries about the processes coupling development of the CNS to its maturation and demise. [**AU: please note that it is not house style to include sub-headings in the discussion. In addition, refs 46 and 47 have been removed and are now included in the Supplementary Information, as they are only referred to in the Supplementary Information. The reference list has now been re-numbered accordingly.**]

METHODS

Western blots. Mice were sacrificed by intraperitoneal-injection of chloral hydrate. Total protein extracts of spinal cord were obtained by homogenization in SDS–urea–β-mercaptoethanol (0.5% SDS and 8 M urea in phosphate buffer at pH 7.4), Triton X-100 lysis buffer (10 mM Tris-HCl at pH 7.5, 150 mM NaCl, 1 mM EDTA at pH 8.0 and 1% Triton X-100) or E1A lysis buffer (50 mM Tris-HCl at pH 7.5, 250 mM NaCl, 5 mM EDTA at pH 8.0 and 0.1% NP-40) with a cocktail of protease inhibitors (phenyl methylsulphonyl fluoride, leupeptin, pepstatin and apoprotinin). The supernatant from the soluble fraction in E1A or Triton X-100 buffer was collected after centrifugation at 10,000*g* for 20 min or 15 min, respectively [**AU: OK?**]. The protein concentration was estimated by the Bradford procedure (BioRad Laboratories, Hercules, CA). Proteins (20–50 μg) were fractionated by SDS–PAGE and blotted onto nitrocellulose or PVDF membranes for western blot analysis. Membranes were incubated with antibodies against NUDEL (210, 211), Lis1, dynein intermediate chain (MAB 1618; Chemicon [**AU: Please include company location. Town and state for US, town and country for non-US**]), actin (C4 and MAB 1501; Chemicon), p50 (C25; BD Transduction Laboratories, [**AU: Please include company location.**]), p150 (C1; BD Transduction Laboratories), NF-L (Alpha-68-DA2; Zymed [**AU: Please include company location.**]; NR-4, AB1983, Chemicon), NF-H (RT-97, NE-14, N-52, AB-1), GST monoclonal (M2, Santa Cruz Biotechnology) and polyclonal (Z5, Santa Cruz Biotechnology), His (6 × His, Clontech), and α-Tubulin (B512, Sigma). Antibodies were detected by RENAISSANCE, a western blot chemiluminescence kit from NEN Life Science (Boston, MA). Quantifications were normalized against levels of actin or α-Tubulin and interpreted using the Labscan program (Image Master, 2D software v 3.10; Amersham Pharmacia biotech).

GST pull down and immunoprecipitation. Purified GST and GST–NUDEL in Buffer E1A were absorbed to glutathione (GSH) beads and cross-linked to the resin with 20 mM DMP (in 0.2 M sodium borate at pH 9.0) for 1 h at 4 °C. Beads were then washed with 0.2 M ethanolamine (at pH 8.0) before washing with E1A lysis buffer. Spinal cords were homogenized in NP-40 lysis buffer, and 500 μg of lysate was incubated with GSH beads cross-linked to 10 μg of GST fusion proteins. Binding of NF proteins to the GST–NUDEL protein was analysed by western blotting. Immunoprecipitations were performed as described[2,4]

Neurofilament preparation. A neurofilament-enriched fraction was prepared from the spinal cord of C57BL6 and NF-L-null mice using a slightly modified version of a procedure described previously[24]. A complete (or half) spinal cord was homogenized in 400 μl of Buffer A (0.1 M NaCl, 1 mM EDTA at pH 8.0 and 10 mM sodium phosphate at pH 6.5) containing 0.85 M sucrose. The volume was then adjusted to 2 ml with Buffer A. The homogenate was centrifuged at 27,000*g* for 15 min, before collection of the floating pad of myelinated axons and re-homogenization in 1.5 ml of Buffer B (0.1 M NaCl, 1 mM EDTA at pH 8.0, 10 mM sodium phosphate at pH 6.5 and 1% Triton X-100). The final homogenate was then added to 500 μl of buffer-B before centrifugation at 27,000 *g* for 1 h. The neurofilament-enriched pellet was resuspended in 50 μl of 1× Laemmli buffer before loading onto SDS–PAGE gels. [**AU: OK?**]

Far-western assay. Neurofilament triplet subunits were purified as previously described [**AU: please indicate a reference here**]. GST–NUDEL (M_r of approximately 70K) and His–NUDEL (M_r of approximately 45K) fusion proteins contain the full-length protein with the α-helical coiled-coil domains and the C-terminal tail. Fusion proteins were expressed in XL-1 Blue *Escherichia coli* (Stratagene, [**AU: Please include company location.**]) cells and purified on an anti-β-galactosidase affinity column or Nickel column (Promega, Madison, WI) according to the manufacturer's protocol. Purified neurofilament triplet proteins (10–50 μg) were resolved on a SDS–PAGE gel, blotted onto nitrocellulose, and cut into strips. The strips were blocked and incubated with 3–5 mg ml^{-1} of GST, GST–NUDEL, His or His–NUDEL protein and controlled with preparations derived from NF-L-null mice. Bound GST–NUDEL was detected with monoclonal or polyclonal anti–GST or anti-NUDEL antibodies. Bound His–NUDEL was detected with monoclonal anti-His antibody or anti-NUDEL antibodies.

Yeast two-hybrid interactions. A human cDNA for full-length (amino acids 1–345), coiled-coil domain (amino acids 12–198) and carboxyl tail (amino acids 191–345) of NUDEL was amplified by PCR and inserted into the *Sal*I and *Not*I sites of the pPC97 vector (pDBLeu; Invitrogen, Carlsbad, CA) for expression as a GAL4-DNA-binding-domain fusion protein (pPC97–NUDEL-FL, pPC97–NUDEL-coil-coil and pPC97–NUDEL-tail, respectively). The pPC86–NFL-rod plasmid for expression of the NFL rod-domain (amino acids 77–364) as a GAL4-activation-domain was a kind gift from M. Ehlers (Duke University) and R. Huganir (John Hopkins University). MaV203 cells [**AU: OK?**]containing *LacZ* and *URA* reporter genes under the control of the GAL4 promoter [**AU: OK?**] were transformed with pPC86–NFL-rod-domain and either pPC97–NUDEL, pPC97–NUDEL-CC, or pPC97–NUDEL-tail sequences[2]. Colonies grown on *Leu*$^-$/*Trp*$^-$ media were streaked onto a YPD [**AU: please define**] plate for β-galactosidase assay and a *Ura*$^-$ plate for growth test (data not shown). Colony-lifting assays for β-galactosidase expression were carried out according to the manufacturer's instructions (Clontech, Palo Alto, CA). [**AU: OK?**]

***In vitro* NF polymerization.** Absorbance changes of neurofilament (NF) solutions were measured during the polymerization process. The measurement was performed on the basis that the formation of polymers in solution causes light scattering. The assembly was monitored at A_{350}. This measurement corresponds to the turbidity measurement of polymerization. Lyophilized bovine spinal cord NF proteins (Sigma) were reconstituted at a concentration of 1 mg ml^{-1} in cold neurofilament assembly buffer containing 40 mM Tris–HCl at pH 6.8, 0.1 mM EDTA, 0.1 mM EGTA and 200 mM NaCl. NF solution was dialysed against the assembly buffer to remove urea at 4 °C [**AU: OK?**] overnight (3 × 4 h dialysis). NF aggregates were removed by centrifugation before the assembly reaction. NF proteins (20 μg), NUDEL (20 μg) or NUDEL-CC (20 μg) were polymerized in 120 μl of assembly mixture. Assembly was initiated when the temperature was switched to 30 °C. Assembly samples (10 μl), described in the NF assembly assay, were spotted onto grids for electron microscopy analysis. After 1 min of the settlement process, the liquid was removed from the grids. Grids were then rinsed twice with 10 μl of warm assembly buffer. The grids were then incubated with 4% uranium acetate for 1 min, followed by a drying process at room temperature overnight, before examination by transmission electron microscopy.

Chymotrypsin digestion. Purified bovine spinal cord NFs suspensions [**AU: OK?**] were assembled at 37 °C according to a standard protocol [**AU: please include a reference**]. The product was treated with sequencing-grade α-chymotrypsin from bovine pancreas (Roche Diagnostics, Mannheim, Germany) at 30 °C for 5 and 10 min, at a dilution of 1:2,500. Digestion was terminated by addition of protein loading buffer.

Culture and immunofluorescence of SW13$^-$ cells, cortical neurons and spinal cord tissues. [**AU: Please shorten Title to fit on one line.**] SW13$^-$ cells were cultured as described[26]. After transfection with Lipofectamine [**AU: Please include company name and location.**], SW13$^-$ cells were washed once in warm PBS before fixation with 4% paraformaldehyde/PBS for 10 min at room temperature. After fixation, cells were washed twice with PBS and blocked with PBS containing 5% skimmed milk and 0.1% Triton X-100 for 1 h. After fixation, cells were incubated with primary antibody (RT-97, NE 14, SMI-32, α-68 or NUDEL) diluted in the blocking buffer for 1 h at 37 °C. After three washes with PBS, secondary antibodies (Alexa-488, -594 [**AU: Please include company name and location.**]) were diluted in blocking buffer and added to the cells for 1 h at 37 °C. Finally, cells were washed three times with PBS followed by a wash with water before mounting with Immuno-Mount [**AU: Please include company name and location.**]. Cortical neurons were isolated, cultured and stained as described[30]. The following primary antibodies were used: anti-NUDEL (210, 211), anti-Lis1, anti-NF-L (α-68-DA2, Zymed; NR-4, MAB 1983 Chemicon) and anti-NF-H (RT-97, N-52). Staining of spinal cord tissues was performed as described[32].

Immunogold labelling. For preparation of cryostections, tissues were fixed in 4% paraformaldehyde. After a minimum of 2 h fixation at room temperature, the fixative was removed and replaced with PBS. Before freezing in liquid nitrogen, tissues were infiltrated with 2.3 M sucrose in PBS for 1–2 h. Frozen samples were sectioned at –120 °C and transferred to formvar-carbon-coated copper grids and floated on PBS until ready for immunogold labelling. The immuno-

gold labelling was performed at room temperature on a piece of parafilm. All antibodies and Protein-A–gold were diluted in 1% BSA. Antibody dilutions were centrifuged at 14,000 rpm [**AU: please express in units of '*g*'**] exactly 1 min before labelling to avoid aggregation. Grids were floated on drops of 1% BSA for 10 min to block non-specific labelling, transferred to 5-μl drops of primary antibody and incubated for 1–2 h. Grids were then washed in four consecutive drops of PBS for a total of 15 min, transferred to 5-μl drops of Protein-A–gold for 20 min, washed in four drops of PBS for a total of 15 min and, finally, washed in six drops of distilled water. After the first incubation of Protein-A gold, grids were washed in four drops of PBS for a total of 15 min. They were then transferred to a drop of 1% glutaraldehyde/PBS for 5 min and washed in four drops of PBS/0.15 M glycine to quench the free aldehyde groups. After this treatment, the secondary antibody was applied for 1–2 h before PBS/distillated water washes and Protein-A gold incubation (see above). Contrast and embedding of the labelled grids were performed on ice with 0.3% uranyl acetate (Electron Miscroscopy Sciences [**AU: Please include company location.**]) and 2% methyl cellulose (Sigma) for 10 min. Excess liquid was removed from the grids by streaking on Whatmann paper, leaving a thin coat of methyl cellulose. The grids were examined with a JEOL 1200 EX transmission electron microscope and images recorded at 20,000–40,000× magnification.

Generation and characterization of RNAi vectors, and *in utero* electroporation. RNAi sequences were selected on the basis of criteria described previously[46]. Complementary hair-pin sequences were synthesized commercially and cloned into pSilencer-2.0 under the control of the U6 promoter (Ambion [**AU: Please include company location.**]). The sequence for *NUDEL*-RNAi is base pairs 276–294 (5′-GCAGGTCTCAGTGTTAGAA-3′). Base-pair mutations on positions 279, 285 and 291 (coding for the same amino acid) were introduced into the sequence of an RNAi-resistant *NUDEL* plasmid (5′-GCAAGTCTCGGT-GTTGGAA-3′) through two rounds of PCR. The sequences for *NF-L*-RNAi is base pairs 427–445 (5′-GCCGAGCTGTTGGTGCTGC-3′; L2) and 1,069–1,087 (5′-TGAGCTGAGAAGCACGAAG-3′; L1). L2 corresponds to a positive control published previously[29]. A random sequence without homology to any known mRNA was used as a control RNAi. All RNAi plasmids were tested in 3T3 cells, CAD cells and primary neuronal cultures by both western blot analysis and immunocytochemical staining. Neurons were transfected with Lipofectamine or electroporated with the nucleotransfection device (Amaxa [**AU: Please include company location.**]). After 2–3 days in culture, cells were lysed in RIPA or 0.5% SDS 8 M urea buffer for western blot analysis, or fixed in 4% paraformaldehyde for immunoassaying. *In utero* electroporation was performed as described[30]. EGFP vector (3 mg ml^{-1}) was co-injected with RNAi vector (6 mg ml^{-1}) at a concentration ratio of 1:6. For triple-electroporation experiments, RNAi-resistant *NUDEL* was prepared at 10 mg ml^{-1}. A mixture of EGFP, RNAi and the third DNA plasmid was prepared at a ratio of 1:3:3 in PBS buffer.

Generation of SOD1^{G37R} transgenic mice and mice with an altered NF background. Transgenic mice overexpressing SOD1^{G37R} (line 29; G37R) and human NF-H [**AU: OK?**]were generated as described [**AU: please include a reference**], and were maintained in a pure C57BL6 background[32,47]. All animals were genotyped by Southern blotting. The lifespan of our SOD1^{G37R} mouse (line 29) in a pure C57BL6 background is approximately 52 weeks. The SOD1^{G37R} mice (line 29) overexpressing the human NF-H protein were produced and characterized previously[32,33]. The use of animals and all surgical procedures described in this article were carried out according to The Guide to the Care and Use of Experimental Animals of the Canadian Council on Animal Care (www.ccac.ca).

Sucrose gradient. High-speed supernatants were made from spinal cord homogenates of 4-month-old pre-symptomatic, end-stage SOD1^{G37R} transgenic mice, wild-type littermates or cell lysates. Samples were resuspended in Buffer A (50 mM Tris–HCl at pH 7.4, 150 mM NaCl and 1 mM EDTA) or RIPA buffer plus protease inhibitors, and fractionated on sucrose gradients. Homogenate (200 μl) was overlaid onto a 12 ml, 5–20% sucrose gradient and centrifuged at 32,000*g* [**AU: OK?**] for 18 h at 4 °C in an ultracentrifuge. Sucrose gradients were made previously by utilizing a gradient maker Hoeffer 15, as described by the manufacturer's protocol (Amersham). During all centrifugations, gradients were loaded with 1 mg of standards, such as bovin serum albumin (BSA), catalase or thyroglobulin, and processed simultaneously. After centrifugation, 12× 1-ml fractions were collected for each sample.

Processing of spinal cord tissues. Mice were sacrificed by overdose of chloral hydrate, perfused with 0.9% NaCl, and then with fixative (4% v/v paraformalhdehyde in PBS buffer, at pH 7.4). Tissues sections were prepared for embedding in parafin, cut and stained with Hematoxylin Eosin or the Bielchowsky silver stain.

RT–PCR. Isolation of RNA from cortical neurons was performed using RNAqueous (Ambion), according to the manufacturer's protocol. RNA samples were quantified by spectroscopy. 100 ng of each sample was used for RT–PCR, which was performed with the Titanium One-Step RT–PCR kit (BD Biosciences, Clontech, CA) under conditions described previously[48]. Pairs of primers for NF-L were designed as described[43]. Pairs of primers for Peripherin and β-actin were designed as described[48].

Note: Supplementary Information is available on the Nature Cell Biology website.

ACKNOWLEDGMENTS

The technical help of P. Hince, S. Millecamps and M. Ericsson is gratefully acknowledged. We are grateful to J. Robertson for the CMV–NF-L and CMV–NF-H [**AU: OK?**] plasmids; M. Elhers and R. Huganir for the pC86–NF-L–rod plasmid; T. Shea for the NF-M–GFP plasmid; A. Musacchio for purified NUDEL-CC; D.L. Price and D.W. Cleveland for the kind gift of SOD1^{G37R} mice (line 29); J. Colhberg and U. Aebi for helpful advice on NF polymerization; Z. Xie and R. Ayala for discussions; and M.-T. A. Nguyen [**AU: OK?**], L. Moy, J. Cruz and B. Samuels for critical reading of the manuscript. This work was supported by grants from the National Institutes of Health (for J.-P.J and L.-H.T.) and the Howard Hughes Medical Institute (for L.-H. T.) M.D.N. held a KM Hunter/CIHR [**AU: please spell out**] PhD scholarship and is a recipient of a long-term fellowship from the Human Frontier Science Program Organization. K.S. holds a JSPS [**AU: please spell out**] postdoctoral fellowship for Research Abroad. R.L. was a recipient of a PhD scholarship from the Fonds de la Recherche de la Santé du Québec. S.-K.P. is a fellow of the Taplin Foundation.

COMPETING FINANCIAL INTERESTS

The authors declare that they have no competing financial interests.

Received 8 MARCH 2004; accepted 27 MAY 2004

Published online at http://www.nature.com/naturecellbiology.

1. Morris, J. A., Kandpal, G., Ma, L. & Austin, C. P. DISC1 (disrupted in schizophrenia 1) is a centrosome-associated protein that interacts with MAP1A, MIPT3, ATF4/5 and NUDEL: regulation and loss of interaction with mutation. *Hum. Mol. Genet.* **12,** 1591–608 (2003).
2. Niethammer, M., Smith, D. S., Ayala, R., Peng, J., Ko, J., Lee, M. S., Morabito, M. & Tsai, L. H. NUDEL is a novel Cdk5 substrate that associates with LIS1 and cytoplasmic dynein. *Neuron* **28,** 697–711 (2000).
3. Sasaki, S., Shionoya, A., Ishida, M., Gambello, M. J., Yingling, J., Wynshaw-Boris, A. & Hirotsune, S. A LIS1/NUDEL/cytoplasmic dynein heavy chain complex in the developing and adult nervous system. *Neuron* **28,** 681–696 (2000).
4. Smith, D. S., Niethammer, M., Ayala, R., Zhou, Y., Gambello, M. J., Wynshaw-Boris, A. & Tsai, L. H. Regulation of cytoplasmic dynein behaviour and microtubule organization by mammalian Lis1. *Nature Cell Biol.* **2,** 767–775 (2000).
5. Toyo-oka, K., Shionoya, A., Gambello, M. J., Cardoso, C., Leventer, R., Ward, H. L., Ayala, R., Tsai, L. H., Dobyns, W., Ledbetter, D., Hirotsune, S. & Wynshaw-Boris, A. 14–3-3ε is important for neuronal migration by binding to NUDEL: a molecular explanation for Miller-Dieker syndrome. *Nature Genet.* **34,** 274–285 (2003).
6. Fuchs, E. & Cleveland, D. W. A structural scaffolding of intermediate filaments in health and disease. *Science* **279,** 514–519 (1998).
7. Julien, J. P. Neurofilament functions in health and disease. *Curr. Opin. Neurobiol.* **9,** 554–560 (1999).
8. Julien, J. P. & Mushynski, W. E. Neurofilaments in health and disease. *Prog. Nucleic Acid Res. Mol. Biol.* **61,** 1–23 (1998).
9. Lariviere, R. C. & Julien, J. P. Functions of intermediate filaments in neuronal development and disease. *J. Neurobiol.* **58,** 131–48 (2004).
10. Lee, M. K. & Cleveland, D. W. Neuronal intermediate filaments. *Annu. Rev. Neurosci.* **19,** 187–217 (1996).
11. Kost, S. A., Chacko, K. & Oblinger, M. M. Developmental patterns of intermediate filament gene expression in the normal hamster brain. *Brain Res.* **595,** 270–280 (1992).
12. Schlaepfer, W. W. & Bruce, J. Simultaneous up-regulation of neurofilament proteins during the postnatal development of the rat nervous system. *J. Neurosci. Res.* **25,** 39–49 (1990).
13. Zhu, Q., Couillard-Despres, S. & Julien, J. P. Delayed maturation of regenerating myelinated axons in mice lacking neurofilaments. *Exp. Neurol.* **148,** 299–316 (1997).
14. Bennett, G. S. & DiLullo, C. Slow post-translational modification of a neurofilament

protein. *J. Cell Biol.* **100,** 1799–1804 (1985).
15. Black, M. M., Keyser, P. & Sobel, E. Interval between the synthesis and assembly of cytoskeletal proteins in cultured neurons. *J. Neurosci.* **6,** 1004–1012 (1986).
16. Rao, M. V., Engle, L. J., Mohan, P. S., Yuan, A., Qiu, D., Cataldo, A., Hassinger, L., Jacobsen, S., Lee, V. M., Andreadis, A., Julien, J. P., Bridgman, P. C. & Nixon, R. A. Myosin Va binding to neurofilaments is essential for correct myosin Va distribution and transport and neurofilament density. *J. Cell Biol.* **159,** 279–290 (2002).
17. Roy, S., Coffee, P., Smith, G., Liem, R. K., Brady, S. T. & Black, M. M. Neurofilaments are transported rapidly but intermittently in axons: implications for slow axonal transport. *J. Neurosci.* **20,** 6849–6861 (2000).
18. Shah, J. V., Flanagan, L. A., Janmey, P. A. & Leterrier, J. F. Bidirectional translocation of neurofilaments along microtubules mediated in part by dynein/dynactin. *Mol. Biol. Cell* **11,** 3495–3508 (2000).
19. Wang, L., Ho, C. L., Sun, D., Liem, R. K. & Brown, A. Rapid movement of axonal neurofilaments interrupted by prolonged pauses. *Nature Cell Biol.* **2,** 137–141 (2000).
20. Yabe, J. T., Pimenta, A. & Shea, T. B. Kinesin-mediated transport of neurofilament protein oligomers in growing axons. *J. Cell Sci.* **112**, 3799–3814 (1999).
21. Helfand, B. T., Chang, L. & Goldman, R. D. The dynamic and motile properties of intermediate filaments. *Annu. Rev. Cell Dev. Biol.* **19,** 445–467 (2003).
22. Helfand, B. T., Chang, L. & Goldman, R. D. Intermediate filaments are dynamic and motile elements of cellular architecture. *J. Cell Sci.* **117,** 133–141 (2004).
23. Jung, C., Yabe, J., Wang, F. S. & Shea, T. B. Neurofilament subunits can undergo axonal transport without incorporation into Triton-insoluble structures. *Cell. Motil. Cytoskeleton* **40,** 44–58 (1998).
24. Julien, J. P. & Mushynski, W. E. The distribution of phosphorylation sites among identified proteolytic fragments of mammalian neurofilaments. *J. Biol. Chem.* **258,** 4019–4025 (1983).
25. Beaulieu, J. M., Jacomy, H. & Julien, J. P. Formation of intermediate filament protein aggregates with disparate effects in two transgenic mouse models lacking the neurofilament light subunit. *J. Neurosci.* **20,** 5321–5328 (2000).
26. Beaulieu, J. M., Robertson, J. & Julien, J. P. Interactions between peripherin and neurofilaments in cultured cells: disruption of peripherin assembly by the NF-M and NF-H subunits. *Biochem. Cell Biol.* **77,** 41–45 (1999).
27. Lee, M. K., Xu, Z., Wong, P. C. & Cleveland, D. W. Neurofilaments are obligate heteropolymers in vivo. *J. Cell Biol.* **122,** 1337–1250 (1993).
28. Fujita, Y., Okamoto, K., Sakurai, A., Gonatas, N. K. & Hirano, A. Fragmentation of the Golgi apparatus of the anterior horn cells in patients with familial amyotrophic lateral sclerosis with SOD1 mutations and posterior column involvement. *J. Neurol. Sci.* **174,** 137–140 (2000).
29. Helfand, B. T., Mendez, M. G., Pugh, J., Delsert, C. & Goldman, R. D. A role for intermediate filaments in determining and maintaining the shape of nerve cells. *Mol. Biol. Cell* **14,** 5069–81 (2003).
30. Xie, Z., Sanada, K., Samuels, B. A., Shih, H. & Tsai, L. H. Serine-732 phosphorylation of FAK by Cdk5 is important for microtubule organization, nuclear movement, and neuronal migration. *Cell* **114,** 469–482 (2003).
31. Julien, J. P. Amyotrophic lateral sclerosis: unfolding the toxicity of the misfolded. *Cell* **104,** 581–591 (2001).
32. Nguyen, M. D., Lariviere, R. C. & Julien, J. P. Deregulation of Cdk5 in a mouse model of ALS: toxicity alleviated by perikaryal neurofilament inclusions. *Neuron* **30,** 135–147 (2001).
33. Couillard-Despres, S., Zhu, Q., Wong, P. C., Price, D. L., Cleveland, D. W. & Julien, J. P. Protective effect of neurofilament-heavy-gene overexpression in motor neuron disease induced by mutant superoxide dismutase. *Proc. Natl Acad. Sci. USA* **95,** 9626–9630 (1998).
34. Hirokawa, N., Glicksman, M. A. & Willard, M. B. Organization of mammalian neurofilament polypeptides within the neuronal cytoskeleton. *J. Cell Biol.* **98,** 1523–1536 (1984).
35. Hisanaga, S. & Hirokawa, N. Structure of the peripheral domains of neurofilaments revealed by low angle rotary shadowing. *J. Mol. Biol.* **202,** 297–305 (1988).
36. Yuan, A., Rao, M. V., Kumar, A., Julien, J. P. & Nixon, R. A. Neurofilament transport *in vivo* minimally requires hetero-oligomer formation. *J. Neurosci.* **23,** 9452–9458 (2003).
37. Carpenter, S. Proximal axonal enlargement in motor neuron disease. *Neurology* **18,** 841–851 (1968).
38. Rouleau, G. A., Clark, A. W., Rooke, K., Pramatarova, A., Krizus, A., Suchowersky, O., Julien, J. P. & Figlewicz, D. SOD1 mutation is associated with accumulation of neurofilaments in amyotrophic lateral sclerosis. *Ann. Neurol.* **39,** 128–131 (1996).
39. Schmidt, M. L., Murray, J., Lee, V. M., Hill, W. D., Wertkin, A. & Trojanowski, J. Q. Epitope map of neurofilament protein domains in cortical and peripheral nervous system Lewy bodies. *Am. J. Pathol.* **139,** 53–65 (1991).
40. Bergeron, C., Beric-Maskarel, K., Muntasser, S., Weyer, L., Somerville, M. J. & Percy, M. E. Neurofilament-light and polyadenylated mRNA levels are decreased in amyotrophic lateral sclerosis motor neurons. *J. Neuropathol. Exp. Neurol.* **53,** 221–230 (1994).
41. Hill, W. D., Arai, M., Cohen, J. A. & Trojanowski, J. Q. Neurofilament mRNA is reduced in Parkinson's disease substantia nigra pars compacta neurons. *J. Comp. Neurol.* **329,** 328–336 (1993).
42. McLachlan, D. R., Lukiw, W. J., Wong, L., Bergeron, C. & Bech-Hansen, N. T. Selective messenger RNA reduction in Alzheimer's disease. *Brain Res.* **427,** 255–261 (1988).
43. Menzies, F. M., Grierson, A. J., Cookson, M. R., Heath, P. R., Tomkins, J., Figlewicz, D. A., Ince, P. G. & Shaw, P. J. Selective loss of neurofilament expression in Cu/Zn superoxide dismutase (SOD1) linked amyotrophic lateral sclerosis. *J. Neurochem.* **82,** 1118–1128 (2002).
44. Morrison, B. M., Shu, I. W., Wilcox, A. L., Gordon, J. W. & Morrison, J. H. Early and selective pathology of light-chain neurofilament in the spinal cord and sciatic nerve of G86R mutant superoxide dismutase transgenic mice. *Exp. Neurol.* **165,** 207–220 (2000).
45. Kong, J. & Xu, Z. Overexpression of neurofilament subunit NF-L and NF-H extends survival of a mouse model for amyotrophic lateral sclerosis. *Neurosci. Lett.* **281,** 72–74 (2000).
46. Sui, G., Soohoo, C., Affar el, B., Gay, F., Shi, Y. & Forrester, W. C. A DNA vector-based RNAi technology to suppress gene expression in mammalian cells. *Proc. Natl Acad. Sci. USA* **99,** 5515–5520 (2002).
47. Wong, P. C., Pardo, C. A., Borchelt, D. R., Lee, M. K., Copeland, N. G., Jenkins, N. A., Sisodia, S. S., Cleveland, D. W. & Price, D. L. An adverse property of a familial ALS-linked SOD1 mutation causes motor neuron disease characterized by vacuolar-degeneration of mitochondria. *Neuron* **14,** 1105–1116 (1995).
48. Lariviere, R. C., Beaulieu, J. M., Nguyen, M. D. & Julien, J. P. Peripherin is not a contributing factor to motor neuron disease in a mouse model of amyotrophic lateral sclerosis caused by mutant superoxide dismutase. *Neurobiol. Dis.* **13,** 158–166 (2003).